Available online at www.sciencedirect.com
SCIENCE DIRECT
Journal of Molecular Spectroscopy 237 (2006) 27–35
Journal of MOLECULAR SPECTROSCOPY
www.elsevier.com/locate/jms

The ν_5 and $2\nu_9$ bands of the ^{15}N isotopic species of nitric acid ($H^{15}NO_3$): Line positions and intensities

A. Perrin [a,*], Robert Mbiaké [b]

[a] Laboratoire Inter-Universitaire des Systèmes Atmosphériques (LISA), CNRS, Université Paris XII, 61 avenue du Général de Gaulle, 94010 Créteil Cedex, France
[b] Centre de Physique Atomique et Moléculaire et Optique Quantique (CEPAMOQ), Université de Douala, B.P. 8580, Cameroun

Received 23 December 2005; in revised form 10 February 2006
Available online 27 March 2006

Abstract

Nitric acid (HNO_3) plays an important role in the Earth's atmosphere as a reservoir molecule of NO_x species. It has a strong infrared signature at 11 μm which is one of the most commonly used for the infrared retrieval of this species in the atmosphere since this spectral region coincides with an atmospheric window. It is therefore essential to have high quality spectral parameters in this spectral region. For the $H^{14}NO_3$ (main) isotopic species, the 11 μm bands were already the subject of numerous extensive studies which involve not only the ν_5 and $2\nu_9$ cold bands but also the first hot bands. The present work is the first high resolution Fourier transform analysis of the 11 μm bands for $H^{15}NO_3$, which is the second most abundant isotopomer of nitric acid [$a \cong 0.00365(7)$]. In this way, the analysis of the ν_5 and $2\nu_9$ cold bands centered at 871.0955 and 893.4518 cm^{-1} was performed, and as for $H^{14}NO_3$, these bands are significantly perturbed since rather strong resonances couple the 5^1 and 9^2 rotational levels. The theoretical model that we used to compute the line positions and line intensities is directly issued from the one which we used recently for $H^{14}NO_3$ [A. Perrin, J. Orphal, J.-M. Flaud, S. Klee, G. Mellau, H. Mäder, D. Walbrodt, M. Winnewisser, J. Mol. Spectrosc. 228 (2004) 375–391]. Actually, for the $H^{15}NO_3$ line positions, the Hamiltonian matrix accounts for the rather strong Fermi and the weaker Coriolis interactions linking the $5^1 \Longleftrightarrow 9^2$ rotational levels. Using this model which accounts correctly for the strong mixing of the 5^1 and 9^2 upper state energy levels, the ν_5 and $2\nu_9$ line intensities for $H^{15}NO_3$ were satisfactorily computed using the ν_5 and $2\nu_9$ transition moment operators achieved previously for the ^{14}N (main) isotopic species. In this way, the transfer of intensities from the ν_5 fundamental (and presumably strong) band to the $2\nu_9$ overtone (and presumably weak) band could be explained for $H^{15}NO_3$ as it was done previously for the ^{14}N (main) isotopic species. Finally, the position of the $H^{15}NO_3$ $\nu_5 + \nu_9 - \nu_9$ hot band was identified at 875.245 cm^{-1}.

Keywords: Nitric acid; Fermi resonance; 11 microns; Line positions and intensities; ^{15}N isotopic species; Stratosphere

1. Introduction

Nitric acid (HNO_3) plays an important role as a "reservoir" molecule for both the NO_x (nitrogen oxides) and HO_x (hydrogen oxides) species in the stratosphere [1]. These radicals are potentially active contributors to the ozone destruction in the stratosphere through catalytic reactions. For this reason, various isotopic species of nitric acid have been the subject of numerous spectroscopic studies (see [2,3] and references therein).

1.1. The $H^{15}N^{16}O_3$ isotopic species of nitric acid

As far as the $H^{15}N^{16}O_3$ isotopic species is concerned, a preliminary set of rotational and centrifugal constants for the ground vibrational state were achieved by Cox et al. [4] by combining results achieved during the analysis of microwave spectra of nitric acid performed within the ground vibrational state ($v = 0$) for eight different isotopic species, namely: $H^{14}N^{16}O_3$ ([5–9] and references therein),

* Corresponding author. Fax: +33 145171564.
E-mail address: Perrin@lisa.univ-paris12.fr (A. Perrin).

0022-2852/$ - see front matter © 2006 Elsevier Inc. All rights reserved.
doi:10.1016/j.jms.2006.02.005

Table 1
Vibrational energies, rotational, and interacting constants for the ground state and for the $\{5^1,9^2\}$ Vibrational states of $H^{15}NO_3$

	$v=0$[a]	5^1	9^2
(a) Vibrational energies and rotational constants for the ground state and for the $\{5^1,9^2\}$ interacting states (in cm^{-1})			
E_V		875.04957(12)	889.49765(19)
A	0.43404236840	0.43379503(220)	0.43366964(250)
B	0.40350995087	0.40334096(150)	0.39809288(250)
C	0.20881569943	0.20793592(140)	0.20844020(140)
$\Delta_K\times10^6$	0.2447850	0.04558(440)	0.36749(840)
$\Delta_{JK}\times10^6$	−0.1500385	0.10690(500)	−0.30963(900)
$\Delta_J\times10^6$	0.29691311	0.253050(730)	0.31616(130)
$\delta_K\times10^6$	0.24998841	0.35216(150)	0.18423(310)
$\delta_J\times10^6$	0.12617436	0.1046358(360)	0.135351(670)
$H_K\times10^{12}$	4.05124	[b]	[b]
$H_{KJ}\times10^{12}$	−3.71103	[b]	[b]
$H_{JK}\times10^{12}$	0.92060	[b]	[b]
$H_J\times10^{12}$	−0.02979	[b]	[b]
$h_K\times10^{12}$	1.727495	[b]	[b]
$h_{KJ}\times10^{12}$	0.04203	[b]	[b]
$h_J\times10^{14}$	−0.2712	[b]	[b]
$L_K\times10^{16}$	−1.2862	[b]	[b]
$L_{KKJ}\times10^{16}$	1.1641	[b]	[b]
$l_K\times10^{16}$	−0.06411	[b]	[b]
$l_{KKJ}\times10^{16}$	0.26642	[b]	[b]
$l_{JJK}\times10^{16}$	−0.16598	[b]	[b]
Fermi		Coriolis	
(b) Interaction constants for the $\{5^1,9^2\}$ interacting states (in cm^{-1})			
F_0	8.530188808[c]	C_y	0[d]
F_J	$-1.622252(640)\times10^{-4}$	C_{xz}	$4.720(120)\times10^{-4}$
F_z	$-1.0137(200)\times10^{-4}$	$C_{xz,z}$	$1.5600(820)\times10^{-7}$
F_{xy}	$-1.2732(120)\times10^{-4}$		

The quoted errors are one standard deviation.
[a] From [11].
[b] Fixed to the ground state value [11].
[c] Fixed to the value of [21] during the present calculation (see text).
[d] Fixed to zero (see text).

$D^{14}N^{16}O3$ [4,5], $H^{15}N^{16}O_3$ [5], $H^{18}O^{14}N^{16}O_2$ [10], *cis*-$H^{16}O^{14}N^{18}O^{16}O$ [10], *trans*-$H^{16}O^{14}N^{18}O^{16}O$ [10], $D^{15}N^{16}O_3$ [10], and *cis*-$H^{16}O^{15}N^{18}O^{16}O$ [10]. More recently, using an extended set of millimeter wave measurements performed for $H^{15}N^{16}O_3$ at the Jet Propulsion Laboratory and at Ohio State University, precise ground state parameters were obtained for $H^{15}N^{16}O_3$ in [11]. These parameters, which are given in the first column of Table 1, were achieved using a Watson type Hamiltonian written with an A-type reduction and in the I^r representation [12].

The vibrational spectrum of $H^{15}N^{16}O_3$ was investigated in detail at low resolution [13]. At high resolution, only the ν_9 (O–H torsion), ν_7 (O–NO_2 bend), ν_6 (O–NO_2 stretch), ν_8 (out of plane NO_2 bend) [14], and ν_2 (NO_2 a-stretch) [15] fundamental bands were the subject of extensive studies. The present analysis describes the first analysis of the ν_5 and $2\nu_9$ interacting cold bands of $H^{15}NO_3$ in the 11 μm spectral region.

1.2. The 11 μm spectral region

At 11 μm, nitric acid exhibits, in a rather clear atmospheric window, a strong signature which is commonly used for the remote sensing of this species both from satellites or balloons [16–19] or from the ground [20]. As far as the $H^{14}NO_3$ (main) isotopic species is concerned, the 11 μm spectral region has been the subject numerous recent studies. For example, the ν_5 and $2\nu_9$ cold bands located at 879.10755 and 896.44675 cm^{-1}, respectively, were investigated in detail by Fourier transform spectroscopy ([21–23] and references therein). In addition, rotational transitions in ν_5 and $2\nu_9$ were measured using centimeter, millimeter, and submillimetter techniques [21,24–26]. Finally, the first hot bands $\nu_5+\nu_9-\nu_9$ [27] and $3\nu_9-\nu_9$ [28,29] located at 885.425 and 830.6 cm^{-1}, respectively, were investigated in detail.

Because $H^{15}N^{16}O_3$ is the second most abundant isotopomer of nitric acid [$a\cong0.00364(7)$ calculated from the isotopic abundances of ^1H, ^{15}N and ^{16}O quoted in [30]], it is interesting to study it to have a complete description of the infrared spectrum of nitric acid at 11 μm. Therefore, the first goal of the present work is to perform the first high resolution study of the ν_5 and $2\nu_9$ cold bands of $H^{15}NO_3$ using a Fourier transform spectrum and to generate a set of accurate line positions and line intensities for this isotopic variant for the atmospheric applications. In addition, it is important to confirm the quality of the theoretical model which was used for $H^{14}N^{16}O_3$ [21] for accounting the resonances for the 5^1 and 9^2 interacting energy levels.

For the present analysis, we used a FTS spectrum which was recorded at Ottawa for the 11 μm bands of the $H^{15}NO_3$ species. The model which was used in the present study for the line position and line intensity calculations for the v_5 and $2v_9$ bands is based mainly on the one used in [21] for the $H^{14}NO_3$ species for the same interacting bands. Therefore, it is necessary to summarize the main scope of this previous ^{14}N study.

1.3. The v_5 and $2v_9$ bands for the $H^{14}NO_3$ main isotopic species

In [21], the line positions and line intensities parameters for v_5 and $2v_9$ were determined from a least squares fit on a large set of experimental data which were either collected in the literature or achieved during the study. These data involve 5^1 and 9^2 infrared energy levels and v_5 and $2v_9$line intensities obtained from the analyses of Fourier transform infrared spectra [21–23] together with a large set of rotational transitions in the 5^1 and 9^2 vibrational states measured by centimeter, millimeter, and submillimeter wave techniques [21,24–26]. The theoretical models which were used to calculate the v_5 and $2v_9$ line positions and intensities account for the very strong resonances which perturb these bands. Actually, the 5^1 and 9^2 wavefunctions are strongly mixed because of these resonances. This is evidenced by the intensity pattern which was observed at 11 μm for $H^{14}NO_3$, since the overtone (and presumably weak) $2v_9$ band is almost as strong as the fundamental (presumably strong) v_5 band with an intensity ratio of $\mathrm{Int}(2v_9)/\mathrm{Int}(v_5) \sim 0.73$. This strong mixing of the wavefunctions is also confirmed by the observed torsional splittings, which affect both the 9^2 and 5^1 energy levels [21,24–26]. The v_9 mode (torsion of the OH bond relative to the NO_2 moiety) is a large amplitude motion which induces splittings of the energy levels. These large amplitude splittings were easily observed by millimeter wave techniques for the rotational transitions in the 9^2 state (as it was expected) and also (surprisingly enough) for rotational transitions in the 5^1state (which corresponds to the low amplitude NO_2 in plane bending mode). Actually, the average ratio of the observed torsional splitting in the 5^1 and 9^2 excited states ~35 MHz/50 MHz is equal to the band intensity ratio of $2v_9$ and v_5 bands proving that both the transfer of band intensity from v_5 to $2v_9$ and of the torsional splitting from 9^2 to 5^1 have their common origin in a strong mixing of the 5^1 and 9^2 wavefunctions [21,24–26].

1.3.1. Line positions

The form of the Hamiltonian matrix which was used for $H^{14}NO_3$ in [21,26] is described in details in Table 2 of [21]. Due to symmetry considerations, both Fermi- and C-type Coriolis resonances are to be considered in the $5^1 \Longleftrightarrow 9^2$ off-diagonal vibrational operators. The resonances between the 5^1 and 9^2 energy levels are indeed very strong, and the rotational operators for both the $v = 5^1$ and $v = 9^2$ vibrational diagonal blocks include non-orthorhombic terms[1] in addition to Watson-type operators written in an I^r representation with an A-type reduction [12]. Finally, the large amplitude torsional splittings for both the 5^1 and 9^2 energy levels were accounted for by the inclusion, in the 9^2 vibrational block *only*, of a torsional operator written within the frame of the IAM (Internal Axis System) approach [31,32].

Table 2
Hamiltonian matrix for the $\{5^1, 9^2\}$ interacting vibrational states of HNO_3

	5^1	9^2
5^1	$H_{5,5}$	c.c
9^2	$H_{99,5} = F + C$	$H_{99,99}$

v-diagonal operators: Rotational operator (Watson's type Hamiltonian, A-type, I^r reduction).

$$H_{v,v} = E_v + A_v J_z^2 + B_v J_x^2 + C_v J_y^2 - \Delta_K^v J_z^4 - \Delta_{JK}^v \boldsymbol{J}^2 J_z^2 - \Delta_J^v J^4 - 2\delta_J^v \boldsymbol{J}^2 J_{xy}^2 - \delta_K^v \left\{ J_z^2, J_{xy}^2 \right\} + \cdots$$

v-off-diagonal operators: $H_{99,5} = F + C$ (Fermi and Coriolis).

$$F = F_0 + F_J \boldsymbol{J}^2 + F_z J_z^2 + F_{xy} J_{xy}^2,$$

$$C = C_y i J_y + C_{xz} \{J_x, J_z\} + C_{xzz} \left\{ J_z^2 \{J_x, J_z\} \right\},$$

with c.c. = complex conjugate; $\{A, B\} = AB + BA$; $J_{xy}^2 = J_x^2 - J_y^2$.

Actually it proved that, among the parameters appearing in the $5^1 \Longleftrightarrow 9^2$ off -diagonal in v blocks of the Hamiltonian matrix (see Table 2) F_0, which is involved at the zero order in the expansion of the Fermi operator, has a major responsibility for the overall observed strong mixing between the 5^1 and 9^2 wavefunctions of $H^{14}NO_3$. This F_0 parameter is difficult to determine from a least squares fit calculation performed using only the set of infrared 5^1 and 9^2 energy levels since F_0 is strongly correlated with the E_5 and E_{99} vibrational energies. On the other hand, the F_0 parameter could be accurately determined from the set $2v_9$ and v_5 rotational transitions of $H^{14}NO_3$ measured by millimeter and submillimeter wave techniques [21,24–26], when using the Hamiltonian model described in [21,26] which accounts for the transfer of the torsional splittings from the 9^2 to the 5^1 energy levels. In this way, the value which was determined in [26], and later on confirmed in [21] is:

$$F_0 = 8.530188808(620)\ \mathrm{cm}^{-1} (\text{in [21]}). \quad (1)$$

1.3.2. Line intensities

The v_5 and $2v_9$ line intensities were computed using the theoretical approach given in [33,34]. In this way the individual line intensity [in cm^{-1}/(molecule cm^{-2})] is written as

$$k_{\tilde{\nu}}^N = \frac{8\pi^3 \tilde{\nu}}{4\pi\varepsilon_0 3hcZ(T)} \left(1 - \exp\left(-\frac{hc\tilde{\nu}}{kT}\right)\right) \exp\left(-\frac{hcE_A}{kT}\right) R_A^B, \quad (2)$$

[1] These non-orthorhombic terms (in $\{J_x, J_z\}$ ...) which are symmetry allowed (xz is the molecular plane) are usually removed for C_s-type molecules by rotational contact transformations leading to an A-type (or S-type) Watson type reduced Hamiltonian [12].

where A and B are respectively the lower and upper levels of the transition, $\tilde{\nu} = (E_B - E_A)/hc$ is the wavenumber of the transition and $Z(T)$ is the total partition function. In this expression, $R_A^B$is the square of the matrix element of the transformed transition moment operator μ'_Z:

$$R_A^B = \left|\left\langle v', J', K'_a, K'_c, \left|\mu'_Z\right|, 0, J'' K''_a K''_c \right\rangle\right|^2, \quad (3)$$

where μ'_Z is the transformed dipole moment operator [33,34], which is expanded as

$$\mu'_Z = |0\rangle {}^5\mu'_Z\langle 5| + |0\rangle {}^{99}\mu'_Z\langle 9^2|, \quad (4)$$

where the 5 and 99 superscripts are quoted for v_5 and $2v_9$, respectively.

For symmetry reasons both A- and B-type transitions can in principle be observed for v_5 and $2v_9$, and up to the first order, the v_5 and $2v_9$ transition moment operators can be written as:

$$\begin{aligned} {}^5\mu'_Z &= \varphi_z {}^5\mu^1_z + \varphi_x {}^5\mu^1_x \\ {}^{99}\mu'_Z &= \varphi_z {}^{99}\mu^1_z + \varphi_x {}^{99}\mu^1_x, \end{aligned} \quad (5)$$

where φ_x and φ_z stand for the direction cosines φ_{Zx} and φ_{Zz}, respectively. Actually, only three transition moment constants ${}^5\mu^1_z$, ${}^{99}\mu^1_z$, and ${}^{99}\mu^1_x$, namely:

$$\begin{aligned} &{}^5\mu^1_z = 0.250132(320)\text{D}, \\ &{}^{99}\mu^1_z = -0.007375(230)\text{D}, \quad {}^{99}\mu^1_x = 0.03068(200)\text{D} \end{aligned} \quad (6)$$

were necessary to reproduce the whole set of extensive line intensities measured for $H^{14}NO_3$ in [22]. In this way, the line intensity calculations lead to the observed ratio $(\text{Int}(2v_9)/\text{Int}(v_5) \sim 0.73)$ for the $2v_9$ and v_5 total band intensities. Since ${}^5\mu^1_z$ is about 10 times larger than both ${}^{99}\mu^1_z$ and ${}^{99}\mu^1_x$, the bulk of the line intensities for the $2v_9$ band is borrowed from the v_5 band through the strong mixing of the 5^1 and 9^2 wavefunctions which was accounted for during the energy levels calculation.

2. Experimental data

The Fourier transform spectrum of $H^{15}N^{16}O_3$ was recorded with a modified [35] Bomem D8.002 spectrometer located at Ottawa. A maximum optical path difference (MOPD) of 443 cm was used, which gives an instrument line shape (ILS) function, without apodization, of about 0.0014 cm^{-1}. The detector was a Cu:Ge photo-conductive device operated at 4 K. Radiation reaching the detector was limited with cooled longwave pass filters. The $H^{15}N^{16}O_3$ isotopic sample (which was purchased from ISOTEC Inc.) was contained in a 30 cm glass and stainless steel multi-pass cell (*f*/4) set for 28 transits. The spectrum was recorded in the 670–950 cm^{-1} region. Filter cut-on was at 7.88 μm (1270 cm^{-1}). The beam splitter was germanium on a KBr substrate. The spectrum was calibrated by introducing 0.01 Torr of OCS. The sample pressure was about 0.04 Torr. A total of 165 scans were co-added for an observation time of about 20 h.

3. Analysis

Fig. 1 gives an overview of the 11 μm region for $H^{15}N^{16}O_3$. From this figure, it is clear that the $2v_9$ band is about four times weaker than the v_5 band (for $H^{14}N^{16}O_3$ the $2v_9$ band is almost as strong as v_5).

According to symmetry considerations, both the v_5 and $2v_9$ bands are hybrid (with both A- and B-type components). In fact, for the ^{14}N (main) isotopic species, only A-type transitions were observed for v_5, whether the $2v_9$ band is mainly an A-type band with only a rather weak

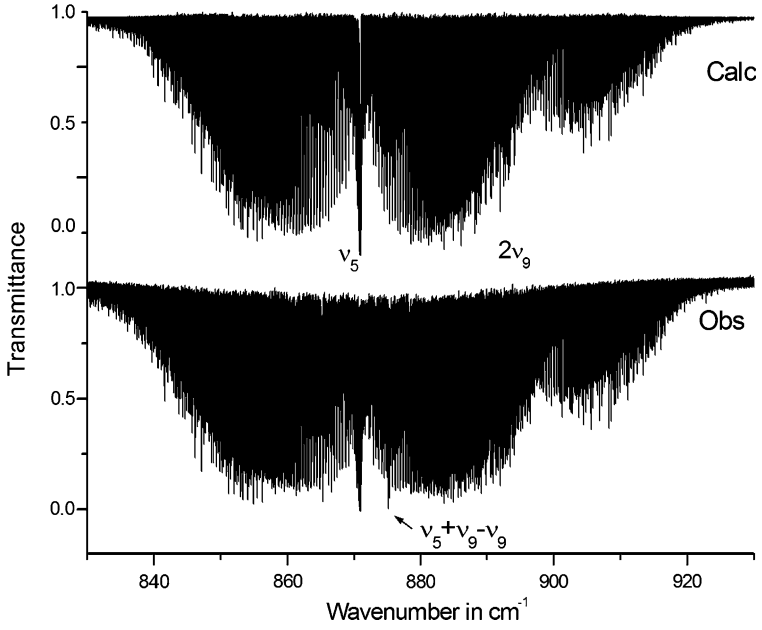

Fig. 1. Overview of the 11 μm region for $H^{15}NO_3$. The v_5 cold band (at 871.0955 cm^{-1}) is significantly stronger than the $2v_9$ cold band (at 893.4517 cm^{-1}). In addition, the sharp *Q* branch of the $v_5 + v_9 - v_9$ can hardly be identified at 875.245 cm^{-1}.

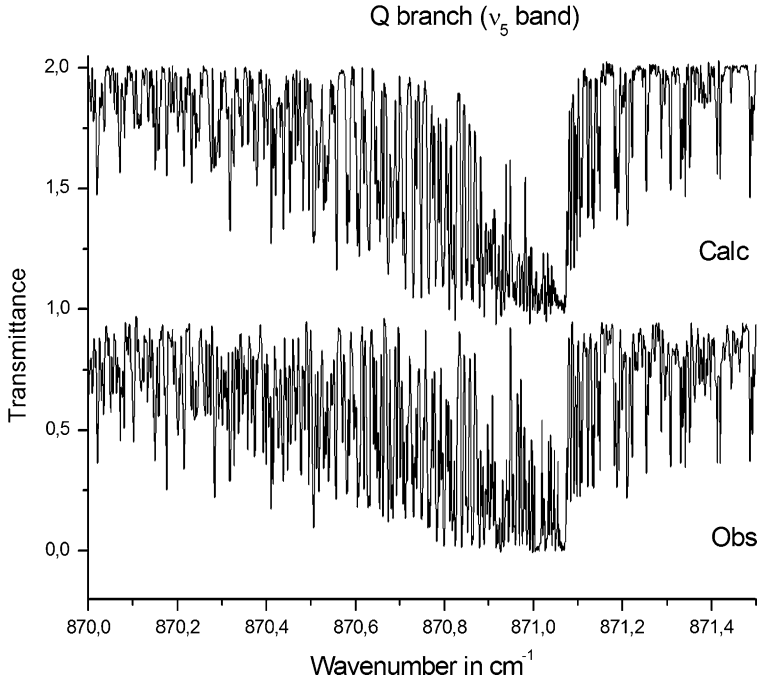

Fig. 2. The Q branch of the ν_5 band around 871.0955 cm^{-1}. Upper trace: line by line calculation. Lower trace: observed spectrum.

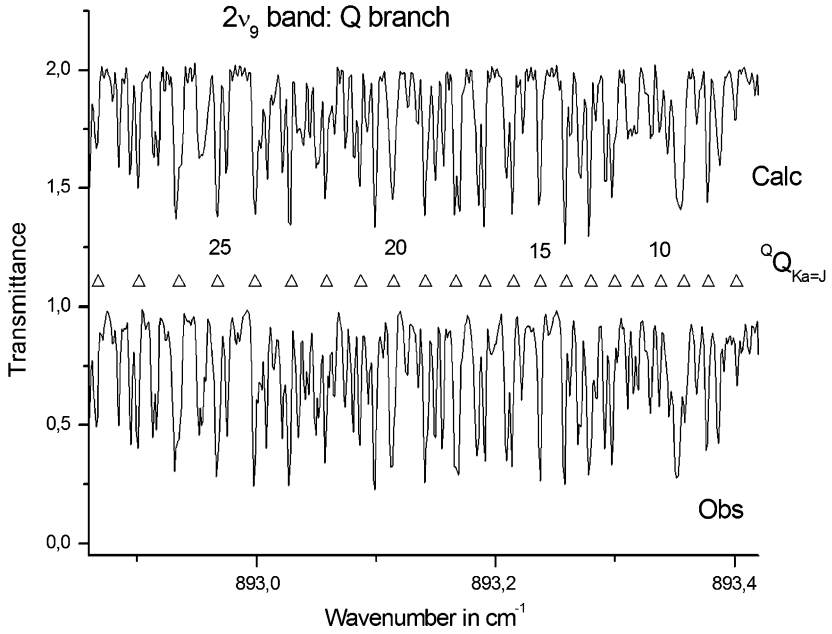

Fig. 3. Part of the Q branch of the $2\nu_9$ band at 925.6 cm^{-1}. Upper trace: line by line calculation. Lower trace: observed spectrum. The quoted assignments are for ^{Q}Q-type transitions with $K'_a = J' - K'_c$ and $K'_c = 0$.

B-type component. In the case of $H^{15}N^{16}O_3$ only A-type transitions were observed for both ν_5 and $2\nu_9$. For A-type transitions, the strongest lines involve $[J, K_a, K_c]$ rotational levels with $K_a \ll K_c \sim J$ in the P and R branches while in the Q branches mainly transitions with $K_c \ll K_a \sim J$ are observable. However, as it can be seen on Figs. 2 and 3 for the ν_5 and $2\nu_9$ bands, respectively, these Q branches are largely congested making the assignments rather difficult.

This analysis was performed in two steps.

First we follow the rather regular series of lines involving low K_a values in the P and R branches and the assignments were checked by ground states combination differences calculated using the lower state rotational constants gathered in the first column of Table 1 [11]. At a given level of the assignments the analysis was complicated because of the existence of local resonances. For example, the rotational energy levels in $K_c = 22$ (respectively in

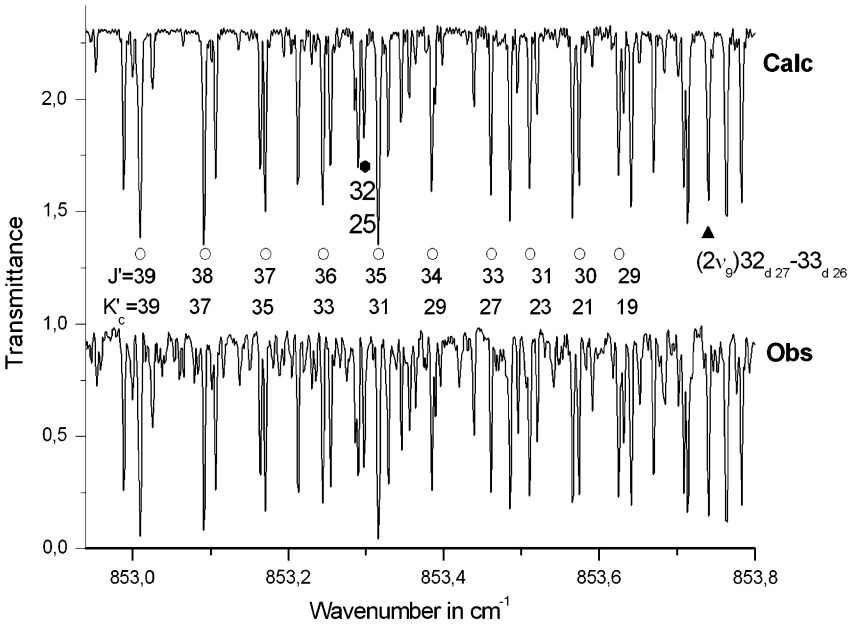

Fig. 4. Portion of the P branch of the v_5 band in the 853.4 cm^{-1} region. Upper trace: line by line calculation. Lower trace: observed spectrum. For this portion of the v_5 P branch, the J' and K'_c upper state rotational quantum numbers are indicated for a series of unresolved doublets ($K_a = J - K_c$ and $K_a = J - K_c + 1$). These v_5 transitions are grouped in a cluster corresponding to ($2J - K_c = 39$). Due to the existence of local vibration rotation resonances linking the rotational levels of the upper 5^1 vibrational state (for $K'_c = 25$) with those of 9^2 (for $K'_c = 27$), the K'_c ordering is somehow perturbed for $K'_c = 25$. Accordingly, the "forbidden" $2v_9$ [32_{d27}–33_{d26}] transition appears at 853.7401 cm^{-1}.

$K_c = 23$, 24, and 25) of the 5^1 vibrational state are strongly interacting with those in $K_c = 24$ (respectively in $K_c = 25$, 26, and 27) of the 9^2 vibrational state, giving rise to a local crossing of the series occurring for $J = 45$ (respectively J = 41, 37, and 32). An example of such resonances is given in Fig. 4. Therefore, the assignments were pursued using the predictions of a theoretical model which accounts for the observed resonances in the system of $\{5^1, 9^2\}$ interacting states and which will be described in the next section.

In total, more than 5500 lines were assigned for the v_5 and $2v_9$ bands. They were added to the ground state energy levels leading to the determination of 1453 and 691 energy levels for the 5^1 and 9^2 vibrational states, respectively, and the maximum J and K_a values are $J = 66$ and $K_a = 31$. Finally, the value achieved for the v_5 band center (871.0955 cm^{-1}) is in good agreement with the value 870.8 cm^{-1} achieved at low resolution in [13].

4. Line positions calculations

4.1. Hamiltonian matrix

The theoretical model which was used in the present study for $H^{15}NO_3$ is somehow deduced from the one used previously for $H^{14}NO_3$ in [21]. Actually, the energy levels calculation for the $\{5^1, 9^2\}$ interacting states must account for the strong Fermi resonances together with somehow weaker C-type Coriolis perturbations. Therefore, the Hamiltonian matrix used in this work to compute the 5^1 and 9^2 energy levels takes the general form which is given in Table 2.

- The H_v^{ROT} rotational operator: For each of the 5^1 and 9^2 states, the H_v^{ROT} rotational operators includes Watson's operator written in an I^r representation with a A-type reduction [12]. On the other hand, and contrary to $H^{14}NO_3$, where these terms had to be considered for both the 5^1 and 9^2 vibrational blocks, it was unnecessary to include non-orthorhombic terms[2] in the v-diagonal blocks. This is because, except in case of local resonances between the 5^1 and 9^2 energy levels, the overall mixing of the 5^1 and 9^2 wavefunctions is significantly weaker for $H^{15}NO_3$ than it was for $H^{14}NO_3$. This is evidenced on Fig. 1 which gives an overview of the 11 μm region for $H^{15}NO_3$ since it is clear in this case that the $2v_9$ band is significantly weaker than the v_5 one.
- The operators off-diagonal in v: Due to symmetry considerations, both Fermi- and C-Coriolis type resonances are to be considered in the off- diagonal operators $H_{99,5}$.

4.2. Results

The least squares fit involves 2144 upper state infrared energy levels. The fit was very satisfactory as can be seen from the statistical analyses given in Table 3 and the obtained standard deviation $0.56 \times 10^{-3} cm^{-1}$ for the infrared levels. The corresponding Hamiltonian constants are given in Table 1 together with their uncertainties. It is worth noticing that these statistical uncertainties do not account for systematic errors. In particular it is estimated that the accuracy on the band centers is not better than 0.0003 cm^{-1}.

Table 3
Statistical analysis of the results of the infrared energy level calculation

	5^1	9^2
Number of levels	1453	691
$0 \leqslant \delta \leqslant 0.5 \times 10^{-3}$ cm^{-1}	89.2%	65.9%
$0.5 < \delta \leqslant 1.5 \times 10^{-3}$ cm^{-1}	8.8%	27.5%
$1.5 \leqslant \delta \leqslant 3.5\text{x}10^{-3}$ cm^{-1}	2.0%	6.6%
Standard deviation (10^{-3} cm^{-1})	0.56	

$\delta = |E_{obs} - E_{calc}|$.

Since there exists no microwave measurements of rotational transitions within the 5^1 and 9^2 states of $H^{15}NO_3$, the F_0 parameter involved at zero order in the expansion of the Fermi-type off diagonal in v operator could not be determined in the present study and was therefore maintained at its value achieved for $H^{14}NO_3$ [see Eq. (1)]. In addition and as for the ^{14}N (main) isotopic species, the parameter involved at the first order in the expansion of the Coriolis operator (in iJ_y) could not be determined from the least squares fit and was maintained at zero. It is important to underline that the rotational constants and centrifugal parameters achieved for the 5^1 and 9^2 vibrational states are purely effective with poor physical meaning. This is evident for example when examining the values achieved for the Δ_K parameter for the 5^1 and the 9^2 vibrational states which are six times weaker and two times stronger, respectively, than the ground state value.

Also important pieces of information which may or may not be obtained from a least squares fit calculation are the absolute signs of the parameters. As usual the signs of all the parameters appearing in the 5^1 and 9^2 rotational Hamiltonians (i.e., the Watson A-type expansions) of the two states under study are obtained from the fit. In addition, the signs of the higher order constants appearing in the Fermi (respectively Coriolis) operator are determined only relative to those of the lower order constant, namely F_0 (respectively C_{xz}). Actually, from the discussion performed in [21] it is clear that the absolute sign of F_0 and C_{xz} cannot be achieved from the present least squares fit, and consequently the signs of the parameters which are given in Table 1 were fixed according to the convention given in [21] for $H^{14}NO_3$:

$$F_0 > 0, \quad C_{xz} > 0. \tag{7}$$

5. Line intensities

As to our knowledge, no experimental data concerning line intensities are presently available for the $H^{15}N^{16}O_3$ isotopic species at 11 μm. Therefore the present line intensity calculations were performed using the transition moment constants (see Eq. (6)) which were achieved for the $H^{14}N^{16}O_3$ isotopic species in [21].

Using the vibrational energies, and the rotational, and coupling constants given in Table 1 for the upper resonating $\{5^1, 9^2\}$ states and for the ground state, together with the transition moment constants given in Eq. (6) we have generated a comprehensive list of line positions and intensities for the $\{v_5, 2v_9\}$ interacting bands. The calculations

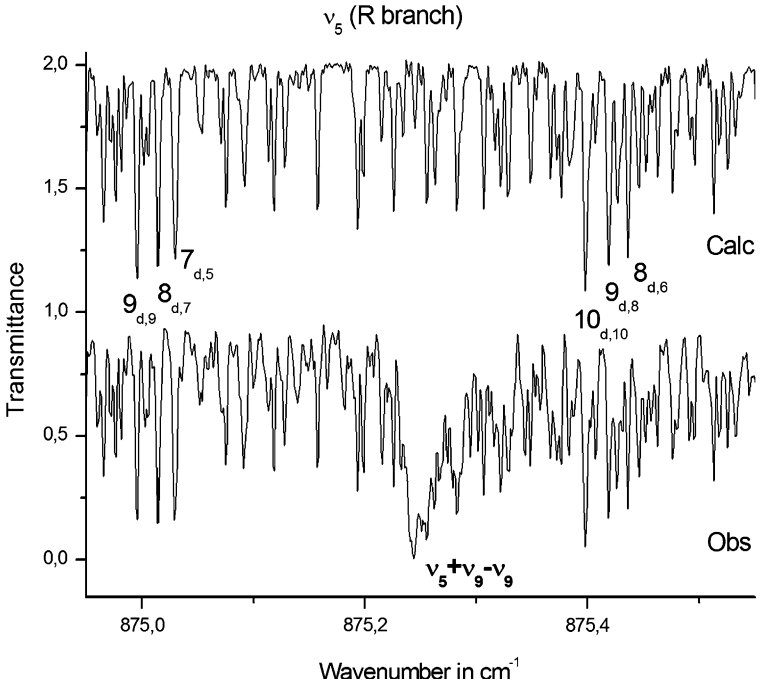

Fig. 5. Part of the spectrum in the 875 cm^{-1} region. Upper trace: line by line calculation. Lower trace: observed spectrum. The $J'_{d'Kc'}$ quoted assignments are given for the upper levels of v_5 A-type transitions (where d stands for degenerate transitions with $K_a = J - K_c$ and $K_a = J - K_c + 1$). The narrow Q branch structure from the $v_5 + v_9 - v_9$ hot band appears clearly at 875.245 cm^{-1}.

were performed at 296 K for a "pure" isotopic sample of $H^{15}N^{16}O_3$ using an intensity cutoff of $0.1\times\ 10^{-22}$cm^{-1}/(molecule cm^{-2}), maximum values of 70 for J and 54 for K_a, maximum lower and upper energies of 2500 cm^{-1} and 3500 cm^{-1}, respectively. For this calculation, we used the following partition function:

$$Z_{\mathrm{vib}}(296\ \mathrm{K}) = 1.30416, \quad Z_{\mathrm{rot}}(296\ \mathrm{K}) = 27196 \quad \text{and therefore} \quad Z(296\ \mathrm{K}) = 35468. \tag{8}$$

In this way, 49,331 lines were computed in the frequency range 813.6 to 934.0 cm^{-1}, and the total band intensities (i.e., the sum of the individual line intensities at 296 K) obtained are $S_{\mathrm{Tot}}(\nu_5) = 1.41\times10^{-17}$ cm^{-1}/(molecule cm^{-2}) and $S_{\mathrm{Tot}}(2\nu_9) = 0.322\times10^{-17}$ cm^{-1}/(molecule cm^{-2}).

Fig. 1 gives an overview of the 11 μm region and it is clear that there is a good overall agreement between the observed and calculated spectra both for the ν_5 and $2\nu_9$ bands. Actually, when using for the $H^{15}NO_3$ isotopic species for the F_0 parameter the value see Eq. (1) which was achieved previously for $H^{14}NO_3$, the transfer of intensity from ν_5 to $2\nu_9$ is significantly weaker for ^{15}N than it was for ^{14}N: in fact, the calculated intensity ratio between the $2\nu_9$ and ν_5 bands intensity is $(\mathrm{Int}(2\nu_9)/\mathrm{Int}(\nu_5)) \sim 0.23$ for $H^{15}NO_3$ instead of ~0.73 for $H^{14}NO_3$. This is because the 5^1 and 9^2 vibrational states are more distant in energy for ^{5}N ($E_5 - E_{99} = 14.4479$ cm^{-1}) than for ^{14}N ($E_5 - E_{99} = 3.0984$ cm^{-1}).

Figs. 2 and 3 give overviews of the Q branches for the ν_5 and $2\nu_9$ bands, respectively. Fig. 4 gives an example of a local resonance which involves near $J = 32$ the $K_c = 25$ series of the 5^1 energy levels with those in $K_c = 27$ of 9^2: in this case also, the agreement between the observed and calculated spectra is satisfactory.

Finally, the present calculation does not account for the hot bands but it was possible to identify the $\nu_5 + \nu_9 - \nu_9$ band at 875.244 cm^{-1} (see Fig. 5). As for the ^{14}N species [26] it exhibits a narrow Q branch structure, and the upper 5^19^1 vibrational state for the $H^{15}NO_3$ isotopic species is estimated at 1453.716 cm^{-1}.

6. Conclusion

Using new Fourier transform spectra recorded in Ottawa, the first analysis of the ν_5 and $2\nu_9$ bands of $H^{15}NO_3$ has been performed. The theoretical models which were used to calculate the line positions and intensities account for the very strong resonances (Fermi and Coriolis), which perturb the 5^1 and 9^2 rotational levels using a model which is directly derived from the one used previously for $H^{14}NO_3$. In this way, it proved possible to generate a significantly improved list of line positions and intensities for the ν_5 and $2\nu_9$ bands of HNO_3. We hope that these results will lead to improve the atmospheric HNO_3 retrievals.

Acknowledgments

The authors are grateful to Dr. John W. Johns from the Steacie Institute for Molecular Sciences (National Research Council of Canada) for providing them the spectrum of $H^{15}NO_3$ which was used during this study. Robert Mbiaké acknowledges gratefully a financial support from the French programs FICU (Fonds International de la Coopération Universitaire) and CORUS (Coopération pour la Recherche Universitaire Scientifique). The authors are deeply indebted to Dr. Jean-Marie Flaud for fruitful discussions and numerous encouragements during the curse of this work.

References

[1] World Meteorological Organization (WMO). Global Ozone Research and Monitoring Project, Rep. 44, Scientific Assessment of Ozone Depletion: 1998. Geneva (1999).
[2] A. Goldman, C.P. Rinsland, A. Perrin, J.-M. Flaud, J. Quant. Spectrosc. Rad. Trans. 60 (1998) 851–861.
[3] A. Perrin, Spectrochim. Acta, Part A A54 (1998) 375–393.
[4] A.P. Cox, M.C. Ellis, C.J. Attfield, A.C. Ferris, J. Mol. Struct. 320 (1994) 91–106.
[5] D. Millen, J.R. Morton, J. Chem. Soc. (1960) 1523–1528.
[6] G. Cazzoli, F.C. De Lucia, J. Mol. Spectrosc. 76 (1979) 131–141.
[7] P.N. Ghosh, C.E. Blom, A. Bauder, J. Mol. Spectrosc. 89 (1981) 159–173.
[8] R.L. Crownover, R.A. Booker, F.C. De Lucia, P. Helminger, J. Quant. Spectrosc. Rad. Trans. 40 (1988) 39–46.
[9] D.T. Petkie, P. Helminger, R.A.H. Butler, S. Albert, F.C. De Lucia, J. Mol. Spectrosc. 218 (2003) 127–130.
[10] A.P. Cox, J.M. Riveros, J. Chem. Phys. 42 (1965) 3106–3112.
[11] B.J. Drouin, C.E. Miller, J.L. Fry, D.T. Petkie, P. Helminger, I.R. Medvedev, J. Mol. Spectrosc. 235 (2006) 293–298.
[12] J.K.W. Watson, Aspects of quartic and sextic centrifugal effects on rotational energy levels, in: J.R. Durig (Ed.), Vibrational Spectra and Structure, Series of Advances, 6, Elsevier, New York, Amsterdam, 1977, p1.
[13] G.E. McGraw, D.L. Bernitt, I.C. Hisatsune, J. Chem. Phys. 42 (1965) 237–244.
[14] F. Keller, A. Perrin, J.-M. Flaud, J.W.C. Johns, Z. Lu, E.C. Looi, J. Mol. Spectrosc. 191 (1998) 306–310.
[15] W.F. Wang, P.P. Ong, H.F. Chen, H.H. Teo, J. Mol. Spectrosc. 185 (1997) 207–208.
[16] J.M. Russell II, C.B. Farmer, C.P. Rinsland, R. Zander, L. Froidevaux, G.C. Toon, B. Gao, J. Shaw, M. Gunson, J. Geophys. Res. D93 (1988) 1718–1736.
[17] H. Oelhaf, T. Von Clarmann, H. Fischer, F. Friedl-Vallon, C. Frizsche, A. Linden, C. Piesch, M. Seefeldner, W. Völker, Geophys. Res. Lett. 21 (1994) 1263–1266.
[18] C. Camy-Peyret, S. Payan, P. Jeseck, Y. Té, C.R. Acad. Sci. Paris, Serie IV 2 (2001) 905–922.
[19] Mencaraglia, F., Bianchini, G., Bosscaleri, A., Carli, B., Ceccherini, S., Raspollini, P., Flaud, J.-M., Perrin, A., J. Geophys. Res., 2005 (accepted).
[20] C.P. Rinsland, R. Zander, P. Demoulin, J. Geophys. Res. D96 (1991) 9379–9389.
[21] A. Perrin, J. Orphal, J.-M. Flaud, S. Klee, G. Mellau, H. Mäder, D. Walbrodt, M. Winnewisser, J. Mol. Spectrosc. 228 (2004) 375–391.
[22] R.A. Toth, L.R. Brown, E.A. Cohen, J. Mol, Spectroscopy 218 (2003) 151–168.

[23] Ch. Chackerian, S.W. Sharpe, T.A. Blake, J. Quant. Spectrosc. Rad. Trans. 82 (2003) 429–441.
[24] T.M. Goyette, Ch.D. Paulse, L.C. Oesterling, F.C. De Lucia, P. Helminger, J. Mol. Spectrosc. 167 (1994) 365–374.
[25] T.M. Goyette, L.C. Oesterling, D.T. Petkie, R.A. Booker, P. Helminger, F.C. De Lucia, J. Mol. Spectrosc. 175 (1996) 395–410.
[26] D.T. Petkie, T.M. Goyette, P. Helminger, H.M. Pickett, F.C. De Lucia, J. Mol. Spectrosc. 208 (1996) 121–135.
[27] J.-M. Flaud, A. Perrin, J. Orphal, Q. Kou, P.M. Flaud, Z. Dutkiewicz, C. Piccolo, J. Quant. Spectrosc. Rad. Trans. 77 (2003) 355–364.
[28] A. Perrin, J.-M. Flaud, C. Camy-Peyret, B.P. Winnewisser, S. Klee, A. Goldman, F.J. Murcray, R.D. Blatherwick, F.S. Bonomo, D.G. Murcray, J. Mol. Spectrosc. 166 (1994) 224–243.
[29] A. Perrin, J.-M. Flaud, C. Camy-Peyret, A. Goldman, C.P. Rinsland, M.R. Gunson, J. Quant. Spectrosc. Rad. Trans. 52 (1994) 319–322.
[30] D.R. Lide (Ed.), CRC Handbook of Chemistry and Physics, 80th ed., CRC Press, Boca Raton, FL, 1999–2000.
[31] J.T. Hougen, J. Mol. Spectrosc. 114 (1985) 395–426.
[32] L.H. Coudert, A. Perrin, J. Mol. Spectrosc. 172 (1995) 352–368.
[33] J.-M. Flaud, C. Camy-Peyret, R.A. TothWater, Vapour Line Parameters from Microwave to Medium Infrared, Pergamon press, Oxford, 1981.
[34] C. Camy-Peyret, J.-M. Flaud, Vibration–rotation dipole moment operator for asymmetric rotors, in: K. Narahari Rao (Ed.), Molecular Spectroscopy Modern Research, 3, Academic Press, New York, 1985, pp. 69–110.
[35] J.W.C. Johns, Mikrochim. Acta [Wien] 3 (1987) 171–188.